PROTEINS: Structure, Function, and Genetics 24:427–432 (1996)

The Role of Helix Formation in the Folding of a Fully α-Helical Coiled Coil

Tobin R. Sosnick,[1] Sharon Jackson,[2] Rosemarie R. Wilk,[2] S. Walter Englander,[1] and William F. DeGrado[1,2]

[1]The Johnson Research Foundation, Department of Biochemistry and Biophysics, University of Pennsylvania, Philadelphia, Pennsylvania 19104-6059 and [2]Chemical & Physical Sciences Department, The DuPont Merck Pharmaceutical Company, Wilmington, Delaware 19880-0328

ABSTRACT **To determine when secondary structure forms as two chains coalesce to form an α-helical dimer, the folding rates of variants of the coiled coil region of GCN4 were compared. Residues at non-perturbing positions along the exterior length of the helices were substituted one at a time with alanine and glycine to vary helix propensity and therefore dimer stability. For all variants, the bimolecular folding rate remains largely unchanged; the unfolding rate changes to largely account for the change in stability. Thus, contrary to most folding models, widespread helix is not yet formed at the rate-limiting step in the folding pathway. The high-energy transition state is a collapsed form that contains little if any secondary structure, as suggested for the globular protein cytochrome c (Sosnick et al., Proteins 24:413–426, 1996).** © 1996 Wiley-Liss, Inc.

Key words: GCN4, protein folding, folding kinetics, helix formation

INTRODUCTION

Many protein folding models envision that secondary structure plays an important role in guiding and promoting early pathway steps.[1–3] If so then helix-stabilizing mutations should accelerate folding, and helix-destabilizing mutations should slow folding. This is rigorously true in two-state folding, as illustrated in Figure 1. To study the role of helix formation in folding, we altered helix propensities at various residue positions in a fully helical molecule and measured the effects on two-state folding and unfolding rates. Only exterior sites of the molecule were substituted to focus specifically on helix formation and avoid complicating context effects.

These experiments used a 33 residue peptide, GCN4-p1, derived from the coiled coil region of the bZIP transcriptional activator GCN4. GCN4-p1 has been shown to experience a two-state equilibrium transition between unstructured monomers[4–7] and a fully α-helical coiled coil dimer[8–11] with an equilibrium constant that depends on peptide concentration, temperature, and solution conditions. To enable kinetic and equilibrium folding reactions to be monitored by fluorescence spectroscopy, we introduced the conservative substitution of a tryptophan residue for tyrosine 17 (GCN4-p1′). The homodimeric coiled coil, GCN4-p1′, with sequence Ac-R-MKQLEDKVEELLSKNWHLENEVARLKKLVGE-R-CONH$_2$ is diagrammed in Figure 2.

MATERIALS AND METHODS

Chemicals

Ultra-pure guanidinium hydrochloride (GdmCl) was purchased from ICN Biomedicals (Aurora, OH), and concentrations were determined by refractometry. All other chemicals were purchased from Fisher Scientific (Fair Lawn, NJ).

Peptide Synthesis

Variants of GCN4-p1′ peptide were prepared and characterized as in Choma et al.[12] Peptide concentrations were determined in 6 M GdmCl using an extinction coefficient for tryptophan at 280 nm of 5,700 M^{-1} cm^{-1}, from Pace et al.[13]

Equilibrium Measurements

Equilibrium values of ΔG° for GCN4-p1′ and the Asp7Gly, Asp7Ala, Ser14Gly, and Ala24Gly variants were determined from GdmCl melting data with circular dichroism spectroscopy at 222 nm using an Aviv 62DS spectrometer and a 2 mm path length cuvet. The ΔG° for Ser14Ala was obtained using fluorescence spectroscopy with a Hitachi 650-10S spectrometer at excitation and emission wavelengths of 285 nm and 355 nm, respectively. Peptide concentrations ranged from 20 to 50 μM at pH 5.5, 100 mM sodium acetate, 10°C.

Stopped-Flow Spectroscopy

Rapid mixing experiments used a Biologic SFM3 stopped-flow apparatus equipped with a 200 W argon/mercury arc lamp and a sample cuvet of 10 mm optical pathlength and 1 mm width. Fluorescence

Received December 29, 1995; accepted December 30, 1995.

Address reprint requests to Tobin R. Sosnick, The Johnson Research Foundation, Department of Biochemistry and Biophysics, University of Pennsylvania, Philadelphia, PA 19104-6059.

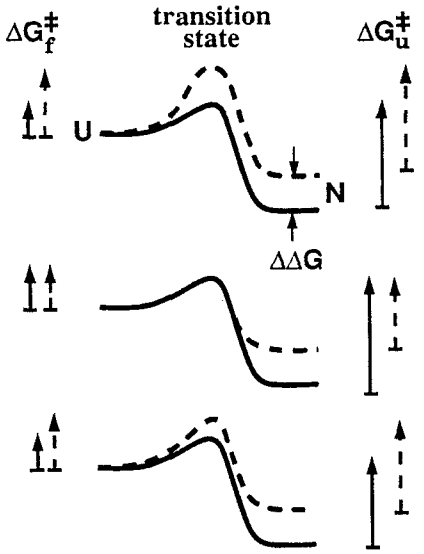

Fig. 1. Free energy diagrams illustrating the possible effects of altered helix stability on folding and unfolding rates. Activation energies for folding and unfolding of the wild-type sequence (solid lines) and variant (dashed lines) are indicated by the height of the arrows. A decrease in equilibrium stability (helical propensity) may be expressed kinetically as a decrease in folding rate (top, $\Phi_f = 1$), an increase in unfolding rate (middle, $\Phi_f = 0$), or a combination of both (bottom, $0 < \Phi_f < 1$) depending on whether helix is present, absent, or partially formed in the transition state at the site of the substitution. The energetic contribution of helical structure to the transition state can be quantified by the Φ_f parameter (Eq. 4) given by $\Delta\Delta G_f^{\ddagger}$, the difference in height of the folding-side arrows, divided by $\Delta\Delta G^{\circ}$, the change in equilibrium stability.

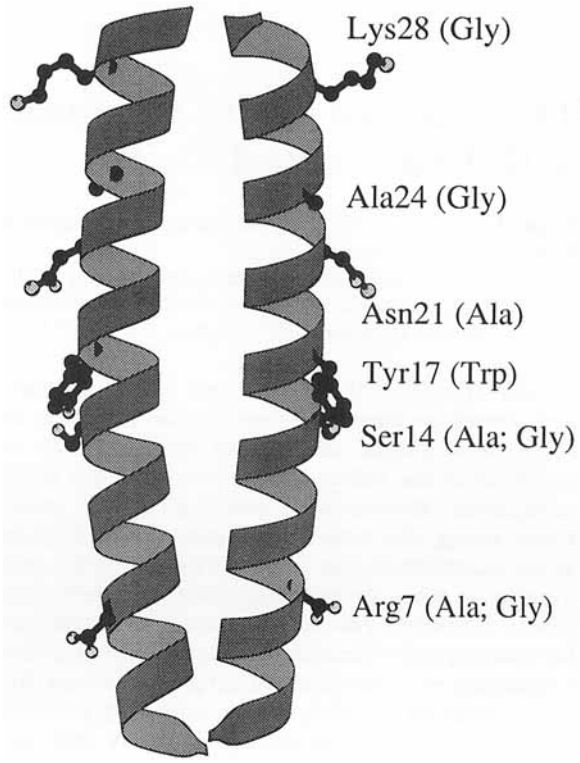

Fig. 2. The GCN4-p1′ homodimer,[8] drawn using MOLSCRIPT.[30] The residue side chains initially present and the substitutions used (parentheses) are shown.

spectroscopy used excitation and emission wavelengths of 267 nm and 300–400 nm, respectively. Temperature control of the sample syringes and observation cuvet was maintained with a circulating water bath. The dead-time of the stopped-flow experiments was 5 msec. Starting from the fully unfolded state (6 M GdmCl) or the folded state (no GdmCl), reactions were initiated by dilution to yield the desired denaturant concentration at pH 5.5, 50–100 mM sodium acetate, 10°C. Peptide concentrations ranged from 5–8 μM. Two to six kinetic traces were averaged at each folding condition.

Data Analysis

The equilibrium data were fit to obtain ΔG° assuming a two-state transition between unstructured monomers and a fully folded dimer, and a linear dependence of ΔG° on denaturant (Eq. 1). Kinetic data were fit using Biologic Biokine software using a Simplex algorithm. Unfolding data were fit to a single exponential equation; refolding data were fit to a second-order bimolecular equation to account for the dependence on protein concentration.[14]

Kinetically determined values for $\Delta\Delta G^{\circ}$ were obtained directly from the kinetic measurements as described in the text except in the case of Ala24Gly where the folding limb could not be accurately specified. For this substitution, $\Delta\Delta G^{\circ}$ was obtained from equilibrium circular dichroism measurements at 222 nm. The displacement of the folding limb was calculated by subtracting the displacement of the unfolding limb, $\Delta\Delta G^{\ddagger}_u$, from $\Delta\Delta G^{\circ}$. Values for Φ_f, defined in Eq. 4, were obtained by a short extrapolation of $\Delta G^{\ddagger}_f$ (see Fig. 4) to zero denaturant concentration.

RESULTS AND DISCUSSION

The folding and unfolding kinetics of GCN4-p1′ can be followed with high sensitivity by the large change in fluorescence intensity of the Trp17 probe residue. When the monomeric random coil form of GCN4-p1′ in guanidinium chloride (GdmCl) is diluted with aqueous buffer, a helical homodimer forms, and Trp17 fluorescence increases by 50%. Folding exhibits second-order bimolecular kinetics (Fig. 3A) with rate proportional to peptide concentration (Fig. 3B), indicating that folding is limited by a reaction that requires monomer-monomer collisions. When the intact GCN4-p1′ dimer is diluted into GdmCl, its fluorescence-detected unfolding exhibits single exponential kinetics (Fig. 3A). The second-order folding and single exponential unfolding behavior indicated by the fluorescence probe agrees with GCN4-p1 folding behavior observed using

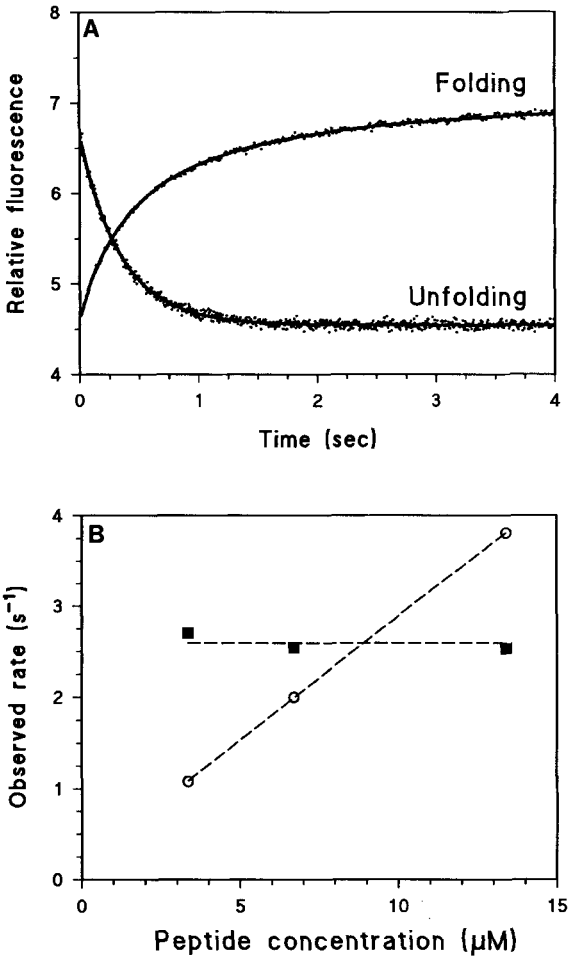

Fig. 3. Folding and unfolding behavior of the Ser14Ala variant (pH 5.5, 10°C). **A:** Solid lines are the second-order fit to the folding data (1.2 M GdmCl) and the single exponential fit to unfolding data (4.8 M GdmCl). In both reactions, the earliest measurable signal is equal to the value for the initial state measured separately, indicating that there is no change in fluorescence signal in the ~ 5 ms instrument deadtime. **B:** The observed initial folding rate, k = k_f[peptide concentration] (○), and the unfolding rate, k_u(■), as a function of peptide concentration. The concentration dependence documents bimolecular folding and unimolecular unfolding. Results for other variants were similar.

stopped-flow circular dichroism[7] but not with the multi-exponential dissociation kinetics seen when otherwise identical chains are tagged with bulky fluorescence transfer probes at their amino termini.[15]

The demonstration of two-state kinetic (and equilibrium) folding and unfolding for GCN4-p1′ described below ensures the validity of the fluorescence probe for measuring folding behavior, since all probes must exhibit the same kinetic behavior in a two-state all-or-none transition.

Helix Content in the Initial Encounter

The folding rate constant found for unmodified GCN4-p1′ when extrapolated to zero denaturant concentration is 2×10^6 M^{-1} s^{-1}, which begins to approach the diffusion-limited rate for monomer collisions,[14,16] ~ 10^9 M^{-1} s^{-1}. This is far too fast to depend on the presence of a large amount of helix prior to collision.

In models that require helix formation prior to collision,[3] the maximum folding rate is the diffusion-controlled rate for chain encounters, ~ 10^9 M^{-1} s^{-1}, multiplied down by the probability that the two colliding monomers are helical. The rate will be even less if all collisions are not productive. The chevron analysis described below shows that a large amount of molecular surface, 55% of the total surface area that is buried in the native coiled coil structure, is buried in the folding transition state ($-m^{\ddagger}_f$ is 50–60% of m^o in all cases). Given the known helical propensities of GCN4-p1′ residues, 55% helix will be present in an average monomer only 10^{-6} of the time (calculated from Zimm-Bragg theory[17] with values for amino acid helical propensities from Chakrabartty et al.[18] and a helix initiation parameter, σ, of 0.001). This quantity of helix will be present in two colliding monomers only 10^{-12} of the time. Thus the maximum folding rate allowed by models that require this much preformed helix to be present at the rate-limiting association step is $(10^{-6})^2 \times 10^9$ M^{-1} s^{-1} = 10^{-3} M^{-1} s^{-1}, slower than the rate observed (10^6 M^{-1} s^{-1}) by 9 orders of magnitude.

This calculation does not include specific stabilizing contributions such as the Asn21 side chain interaction indicated below, worth ~ 1 kcal/mol, which could increase the individual helical probability by perhaps fivefold. Nevertheless, to achieve the folding rates actually observed, this kind of calculation limits helix formation prior to productive collision to less than two turns on both chains (not necessarily in register) or three sequential turns on a single chain.

This rate-based calculation refers to helix present at the initial monomer-monomer encounter step and does not rule out the formation of additional helix in the transition state, after collision. The amount of structure that is present in the transition state can be explored by taking advantage of the two-state nature of GCN4-p1′ folding and the sensitivity of folding to helix stabilizing and destabilizing residues.

Two-State Folding

Measurement of the dependence of folding and unfolding on denaturant concentration provides a rigorous test for the two-state nature of these reactions[7] and also provides a means for the quantitative evaluation of mutational effects. The

TABLE I. Equilibrium and Kinetic Parameters for Dimerization*

	Equilibrium		Kinetic			
Variant	ΔG°	m°	ΔG°	m°	$-m^{\ddagger}_f$	$m^{\ddagger}_u$
GCN4-p1′	10.5 ± .1	1.8 ± .1	10.2 ± .1	1.6 ± .1	0.93 ± .04	0.72 ± .03
Asp7Gly	8.7 ± .2	1.8 ± .1	8.7 ± .1	1.5 ± .1	0.80 ± .08	0.72 ± .04
Asp7Ala	9.4 ± .1	1.6 ± .1	9.9 ± .2	1.5 ± .1	0.75 ± .07	0.71 ± .04
Ser14Gly	8.4 ± .1	1.6 ± .1	9.0 ± .1	1.5 ± .1	0.90 ± .09	0.61 ± .02
Ser14Ala	10.6 ± .6	1.7 ± .2	10.9 ± .1	1.7 ± .04	0.95 ± .03	0.77 ± .02
Asn21Ala			10.5 ± .2	1.7 ± .1	0.96 ± .08	0.78 ± .02
Ala24Gly	8.5 ± .2	2.0 ± .1				0.85 ± .02
Lys28Gly			8.91 ± .1	1.4 ± .02	0.74 ± .02	0.64 ± .01

*Units are kcal/mol for ΔG° and kcal/mol·Mm for m values. The equilibrium determination of ΔG° (extrapolated to zero denaturant concentration and 1 M standard state peptide concentration) and m° values is from equilibrium unfolding experiments and Eq. 1. The kinetic determination of ΔG° and m° values is from the difference between the unfolding and folding activation parameters, using Eqs. 2a,b. The observed agreement documents the two-state nature of the unfolding and folding reactions. Ambient conditions are as in Figure 3.

dependence on GdmCl of the unfolding equilibrium constant, K_u, and the equilibrium stability, ΔG°, is commonly described by a linear relationship.[19]

$$\Delta G^\circ(\text{GdmCl}) = -RT \ln K_u(\text{GdmCl}) = -RT \ln K_u(0) - m^\circ[\text{GdmCl}] \quad (1)$$

Eqs. 2a,b describes the analogous dependence of the activation free energy for kinetic folding (f) and unfolding (u) reactions.

$$\Delta G^{\ddagger}_f(\text{GdmCl}) = -RT\ln k_f(0) - m^{\ddagger}_f[\text{GdmCl}] + \text{constant} \quad (2a)$$

$$\Delta G^{\ddagger}_u(\text{GdmCl}) = -RT\ln 2k_u(0) - m^{\ddagger}_u[\text{GdmCl}] + \text{constant} \quad (2b)$$

Here m° is proportional to the denaturant-sensitive surface exposed on equilibrium unfolding, and $-m^{\ddagger}_f$ and $m^{\ddagger}_u$ are proportional to the surface exposed on moving from either initial state to the transition state.[20,21] The denaturant dependence of two-state kinetic folding and unfolding reactions produces a V- or chevron-shaped curve [20] with its vertex at the midpoint of the equilibrium transition (Fig. 4). The slopes of the left and right limbs of the chevron are the $m^{\ddagger}_f$ and $m^{\ddagger}_u$ surface exposure parameters.

When equilibrium and kinetic folding and unfolding are all two-state reactions limited by the same barrier, then the equilibrium parameters, ΔG° and m°, can be calculated from kinetic measurements according to Eqs. 3, which derives from Eqs. 1 and 2.[14]

$$\Delta G^\circ(0) = -RT\ln(2k_u(0)/k_f(0)) \quad (3a)$$

$$m^\circ = m^{\ddagger}_u - m^{\ddagger}_f \quad (3b)$$

Table I shows values for ΔG° and m° determined for the GCN4-p1′ variants used here. The equivalence of ΔG° and m° values from equilibrium measurements (both circular dichroism at 222 nm and fluorescence) with the values determined independently from kinetic experiments rigorously demonstrates the applicability of a two-state model for GCN4-p1′ folding. This provides a firm basis for studying the transition state.

Helix Content in the Transition State

To test for the presence of helix in the transition state, kinetic experiments were done with amino acid variants of GCN4-p1′ having altered helix propensities. To avoid complicating effects associated with helix-helix packing, only residues at the exterior "f" and "b" positions of the coiled coil were substituted (Fig. 2). If helix propensity is altered at an exterior, non-interacting site that is necessarily helical in the transition state as well as in the native coiled coil, then the free energy of both states will be altered equally, $\Delta\Delta G^{\ddagger}_u$ will equal zero, and the unfolding rate will not change (Fig. 1, top). The entire change in dimer stability will appear in the folding rate, since $\Delta\Delta G^{\ddagger}_f = \Delta\Delta G^\circ$. Other situations will produce different results, as suggested in Figure 1.

To maximize the spread in helical stability, mutant pairs of high and low helix propensity were created. For residues at positions 7, 14, 21, and 24, comparisons were made between a stabilizing alanine and a destabilizing glycine (one substitution in any given peptide). Also the stabilizing residue Lys28 was compared with Gly28. For each variant position studied, the effect found on equilibrium dimer stability (Table I) matches the known difference in helix propensity of the substituted residues.[22] An exception occurs at Asn21 where the substitution of a stabilizing alanine for the destabilizing asparagine produces essentially no change in stability, suggesting that Asn21 participates in a stabilizing context-dependent side chain interaction.

The kinetic results in Figure 4 qualitatively show that these large changes in helix propensity have little effect on the folding rate. The effect of each mutation can be quantified by the parameter Φ_f.[23] As defined in Eq. 4, Φ_f compares the change in stability of the folding transition state, $\Delta\Delta G_f^{\ddagger}$ (displacement of the folding limb of the chevron), with

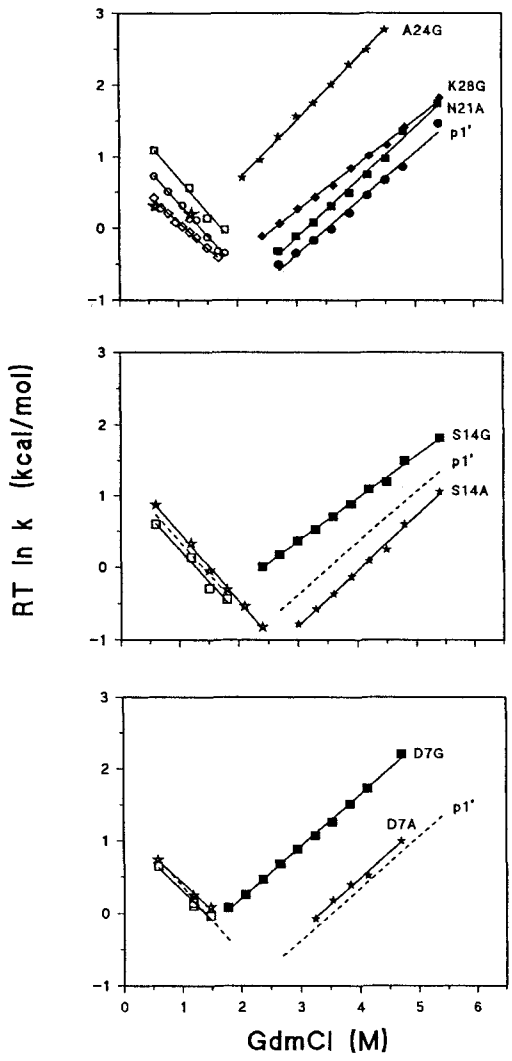

Fig. 4. Denaturant dependence of apparent folding rates (k_{app}, open symbols) and unfolding rates (k_u, closed symbols) for GCN4-p1′ and the variants indicated. Measured bimolecular folding rates have been scaled slightly to conform to a uniform 5.5 μM peptide concentration using the concentration dependence demonstrated in Figure 3B.

the change in equilibrium dimer stability, $\Delta\Delta G^\circ$ (difference between the folding and unfolding displacements).

$$\Phi_f = \Delta\Delta G_f^{\ddagger}/\Delta\Delta G^\circ \quad (4)$$

For the surface substitutions used here in which the change in dimer stability results solely from a change in helix propensity, Φ_f is expected to vary between 0 and 1, reflecting the amount of helical structure that is present at the substituted site in the transition state.

For positions 7, 14, 24, and 28, the measured Φ_f values are 0.06 ± 0.10, 0.15 ± 0.07, 0.26 ± 0.10, and 0.36 ± 0.06, respectively. (These represent Ala to Gly single site comparisons, except at position 28, which is for Lys to Gly.) These low values show that at each substituted position the major fraction of the molecular population lacks well-defined helical structure in the folding transition state(s) (middle and bottom panels in Fig. 1).

More generally, the insensitivity of folding rates to the glycine substitutions indicates that little rigid structure of any kind is formed in the transition state. The low helix propensity of glycine primarily reflects an enhanced stability of the unfolded state due to main-chain conformational freedom at glycine residues and its loss upon helix formation.[24] The lack of effect on the folding rate of GCN4-p1′ when glycine is incorporated shows that the unfolded state and the transition state experience about the same increase in entropic stability. If the substituted residue were constrained in any way in the transition state, even if not in a helical conformation, the transition state would be higher in free energy (less stable) and folding rates would be slowed accordingly.

The Φ_f values found here are small but are not zero, especially near the carboxy-terminus, indicating that the free energy gap between the unfolded state and the transition state is affected in some measure by the substitutions. These low-level effects may indicate either that the residues tested are partially constrained in the transition state, or that they are largely constrained, perhaps even helical, in the transition state but only in a fraction of a heterogeneous population of transition states. A subcategory of the latter pictures the optional nucleation of helix at alternative positions along the chain. If a destabilizing mutation is present at a given position, another region could then serve to nucleate helix formation so that the folding rate is only fractionally affected. As noted before, the presence of two pre-existing turns of helix is allowed by the rate data found. However, the low Φ_f values found at the center of the polymer (Φ_f is 0.14 for Ala14Gly) rules out the general possibility that the polymer contains extensive amounts of variably located helical structure.

CONCLUSIONS

These results and considerations allow only a small population of helix at any given chain position in the transition state for GCN4-p1′ folding. Since the large-scale burial of surface observed in the transition state ($m^{\ddagger}_f/m^0 \sim 0.55$) cannot be accounted for by helix formation, it appears that many non-helical associations must contribute importantly. The glycine substitution results additionally point to considerable flexibility in the transition state. Thus the high-energy transition state is a condensed form that contains a large quantity of loose side chain clustering but little if any secondary structure, with perhaps a small helix initiation site. This view is similar to the transition state described for the two-state folding of the globular protein, cy-

tochrome c,[25] which also involves a large-scale burial of many side chain groups in a loosely defined collapsed form.

The fact that an ideal candidate, a system composed only of two long helices in its native conformation, does not form extensive helix before or during the rate-limiting step as required by most folding models raises an interesting question. Might secondary structure also form late, after the transition state, in the folding of globular proteins? Results for cytochrome c folding leave open the possibility that some helical structure might be present in the transition state.[25] An extensive Φ analysis for barley chymotrypsin inhibitor 2, which also folds rapidly in a two-state manner, shows that this globular protein has little or no secondary structure at the transition state.[26,27] Similarly, the substitution of many sites (one at a time) by helix propensity-altering alanine throughout the largely helical P22 Arc repressor caused little change in folding rates.[28] All these results are consistent with the absence of much secondary structure before or within the folding transition state.

In considering whether secondary structure may generally form relatively late in protein folding, it will be important to focus on two-state folding, where the transition state appears to represent an early intrinsic folding event,[25] rather than on multistate folding, in which the late rate-limiting barrier may well represent a non-intrinsic misfold-reorganization event.[29]

ACKNOWLEDGMENTS

We thank J. Lear, L. Mayne, and R. L. Baldwin for useful discussions and comments on the manuscript, and L. Mayne for assistance in the Zimm-Bragg calculations. This work was supported by research grant GM31847 from the National Institutes of Health.

NOTE ADDED IN PROOF

Similar results obtained for cross-linked variants of GCN4-p1′ affirm the relevance to monomolecular folding of the dimer system used here.

REFERENCES

1. Ptitsyn, O.B. Protein folding: Hypotheses and experiments. J. Protein Chem. 6:273–293, 1987.
2. Kim, P.S., Baldwin, R.L. Intermediates in the folding reactions of small proteins. Annu. Rev. Biochem. 59:631–660, 1990.
3. Karplus, M., Weaver, D.L. Protein folding dynamics: The diffusion-collision model and experimental data. Protein Sci. 3:650–668, 1994.
4. O'Shea, E.K., Rutkowski, R., Kim P.S., Alber, T. Evidence that the leucine zipper is a coiled coil. Science 243:538–542, 1989.
5. Thompson, K.S., Vinson, C.R., Freire, E. Thermodynamic characterization of the structural stability of the coiled-coil region of the bZIP transcription factor GCN4. Biochemistry 32:5491–5496, 1993.
6. Lumb, K.J., Carr, C.M., Kim, P.S. Subdomain folding of the coiled coil leucine zipper from the bZIP transcription activator GCN4. Biochemistry 33:7361–7367, 1994.
7. Zitzewitz, J.A., Bilsel, O., Luo, J., Jones, B.E., Matthews, C.R. Probing the folding mechanism of a leucine zipper peptide by stopped-flow circular dichroism spectroscopy. Biochemistry 34:12812–12819, 1995.
8. O'Shea, E.K., Klemm, J.D., Kim P.S., Alber, T. X-ray structure of the GCN4 leucine zipper, a two-stranded parallel coiled coil. Science 254:539–544, 1991.
9. Oas, T.G., McIntosh, L.P., O'Shea, E.K., Dahlquist, F.W., Kim, P.S. Secondary structure of a leucine zipper determined by nuclear magnetic resonance spectroscopy. Biochemistry 29:2891–2894, 1990.
10. Saudek, V., Pastore, A., Morelli, M.A., Frank, R., Gausepohl, H., Gibson, T. The solution structure of a leucine-zipper motif peptide. Protein Eng. 4:519–529, 1991.
11. Vieth, M., Kolinski, A., Brooks III, C.L., Skolnick, J. Prediction of the folding pathways and structure of the GCN4 leucine zipper. J. Mol. Biol. 237:361–367, 1994.
12. Choma, C.T., Lear, J.D., Nelson, M.J., Dutton, L.P., Robertson, D.E., DeGrado, W.F. Design of a heme-containing four-helix bundle. J. Am. Chem. Soc. 116:1994.
13. Pace, C.N., Vajdos, F., Fee, L., Grimsley, G., Gray, T. How to measure and predict the molar absorption coefficient of a protein. Protein Sci. 4:2411–2423, 1995.
14. Milla, M.E., Sauer, R.T. P22 Arc repressor: Folding kinetics of a single-domain, dimeric protein. Biochemistry 33: 1125–1133, 1994.
15. Wendt, H., Baici, A., Bosshard, H.R. Mechanism of assembly of a leucine zipper domain. J. Am. Chem. Soc. 116: 6973–6974, 1994.
16. Mo, J., Holtzer, M.E., Holtzer, A. Kinetics of self-assembly of alpha-alpha tropomyosin coiled coils from unfolded chains. Proc. Natl. Acad. Sci USA 88:916–920, 1991.
17. Zimm, G.H., Bragg, J.K. Theory of the phase transition between helix and random coil in polypeptide chains. J. Chem. Phys. 31:526–535, 1959.
18. Chakrabartty, A., Kortemme, T., Baldwin, R.L. Helix propensities of the amino acids measured in alanine-based peptides without helix-stabilizing side-chain interactions. Protein Sci. 3:843–852, 1994.
19. Pace, C.N. The stability of globular proteins. CRC Crit. Rev. Biochem. 3:1–43, 1975.
20. Matthews, C.R. Effects of point mutations on the folding of globular proteins. Methods Enzymol. 154:498–511, 1987.
21. Jackson, S.E., Fersht, A.R. Folding of chymotrypsin inhibitor 2. 1. Evidence for a two-state transition. Biochemistry 30:10428–10435, 1991.
22. O'Neil, K.T., DeGrado, W.F. A thermodynamic scale for the helix-forming tendencies of the commonly occurring amino acids. Science 250:646–651, 1990.
23. Fersht, A.R., Matouschek, A., Serrano, L. Folding of an enzyme I. Theory of protein engineering analysis of stability and pathway of protein folding. J. Mol. Biol. 224:771–782, 1992.
24. D'Aquino, J.A., Gomez, J., Hilser, V.J., Lee, K.H., Amzel, L.M., Freire, E. The magnitude of the backbone conformational entropy change in protein folding. Proteins 24:00–00, 1996.
25. Sosnick, T.R., Mayne, L., Englander, S.W. Molecular collapse: The rate-limiting step in two-state cytochrome c folding. Proteins 24:413–426, 1996.
26. Jackson, S.E., elMasry, N., Fersht, A.R. Structure of the hydrophobic core in the transition state for folding of chymotrypsin inhibitor 2: A critical test of the protein engineering method of analysis. Biochemistry 32:11270–11278, 1993.
27. Otzen, D.E., Itzhaki, L.S., elMasry, N.F., Jackson, S.E., Fersht, A.R. Structure of the transition state for the folding/unfolding of the barley chymotrypsin inhibitor 2 and its implications for mechanisms of protein folding. Proc. Natl. Acad. Sci. USA 91:10422–10425, 1994.
28. Milla, M.E., Brown, B.M., Waldburger, C.D., Sauer, R.T. P22 Arc repressor: Transition state properties inferred from mutational effects on the rates of protein unfolding and refolding. Biochemistry 34:13914–13919, 1995.
29. Sosnick, T.R., Mayne, L., Hiller, R., Englander, S.W. The barriers in protein folding. Nature Struct. Biol. 1:149–156, 1994.
30. Kraulis, P.J. MOLSCRIPT: A program to produce both detailed and schematic plots of proteins structures. J. Appl. Crystallogr. 24:946–950, 1991.